General Disclaimer

One or more of the Following Statements may affect this Document

- This document has been reproduced from the best copy furnished by the organizational source. It is being released in the interest of making available as much information as possible.

- This document may contain data, which exceeds the sheet parameters. It was furnished in this condition by the organizational source and is the best copy available.

- This document may contain tone-on-tone or color graphs, charts and/or pictures, which have been reproduced in black and white.

- This document is paginated as submitted by the original source.

- Portions of this document are not fully legible due to the historical nature of some of the material. However, it is the best reproduction available from the original submission.

MEASUREMENT OF THE PRIMARY COSMIC ELECTRON SPECTRUM FROM 10 TO ABOUT 250-GeV

ROBERT F. SILVERBERG

AUGUST 1975

GODDARD SPACE FLIGHT CENTER
GREENBELT, MARYLAND

Measurement of the Primary Cosmic Electron Spectrum

from 10 to about 250 GeV

Robert F. Silverberg
Laboratory for High Energy Astrophysics
NASA/Goddard Space Flight Center
Greenbelt, Maryland 20771

ABSTRACT

The intensity and energy spectrum of primary cosmic electrons from 10 to ~ 250 GeV has been studied using balloon-borne detectors. Both of the detectors were large area ionization calorimeters with frequent sampling of showering particles and were capable of energy resolution of ~ 7%. On one of the flights, a time-of-flight system and detectors to sample the lateral properties of showers were used to examine and improve background rejection. The results of the balloon flights from Alamogordo, N. M. in 1970 and Cape Girardeau, Missouri in 1972 indicated that the primary cosmic ray electron differential energy spectrum exhibits no change of slope in the energy range measured and is well represented by a power law,

$$\frac{dJ}{dE} = (430 \pm 110)E^{-3.10 \pm 0.08} \text{electrons/m}^2\text{-ster-sec-GeV}$$

These results indicate that the cosmic electron spectrum is steeper than the cosmic ray proton spectrum. It is shown that these data are consistent with the leakage lifetime model for the propagation of cosmic electrons in the Galaxy, although other more complex models cannot be excluded on the basis of these data.

i

ACKNOWLEDGEMENTS

INTRODUCTION

Although the composition and energy spectrum of cosmic ray
electrons has been intensively studied for more than a decade, an
experimental consensus on neither the shape of the spectrum nor the
absolute intensity has been achieved   (see e.g. Webber, 1973). Widely
disparate results have been reported using nuclear emulsions (Marar, et al.,
1971; Nishimura et al., 1969; and Anand et al., 1973), and non-visual
techniques (Earl et al., 1972, Müller and Meyer, 1973). Since a wide
variety of results can be found within the same classes of detector, the
discrepancies cannot be attributed to any inherent properties of the
measuring devices. Any attempt to imply a time variation in the high
energy cosmic electron spectra can be dismissed since those experimenters
repeating their work have, in general, confirmed their own results and thus
are observing a consistent electron spectrum above ~ 10 GeV, even though
the inter-experiment results differ.

The basic difficulties at high energies are reliable energy estimation
and elimination of nuclear particles that may masquerade as electrons.
Nuclear emulsions may give unambiguous particle identification, but suffer
from poor energy resolution. On the other hand, ionization spectrometers,
while usually having better energy resolution, eliminate the nuclear back-
ground statistically. Detectors using so called "guard counters" have tended
to report rather low electron intensities (Webber and Rockstroh, 1973
Marar et al., 1971, Muller and Meyer, 1973). Although these low results
may be due to excellent background rejection, they also may be caused
by some rejection of real electron events since the spatial properties
of high energy electron events are generally extrapolated from low energy

accelerator data. We have flown a modified version of the electron

detectors reported previously (Silverberg et al., 1973). The modifi-

cations have included the addition of scintillators to examine the

lateral development of showers and a time-of-flight measuring system

to further exclude any contamination from out of geometry triggers

and other background.

Although five flights were initiated, only three of these, the first,

third and fifth resulted in a significant accumulation of useful data,

the bulk of the high quality data coming from the third and fifth flights.

This paper discusses the last flight in detail and summarizes the

results from the entire series of flights.

DESCRIPTION OF THE DETECTOR

The detector used on the fifth flight can be logically divided into

two portions: the charge section and the electromagnetic cascade section.

The charge section consisted of two plastic scintillators, each 50 x 50 x

0.64 cm and two Cerenkov counters. The uppermost Cerenkov counter (C1)

was a sheet of Pilot 425 measuring 50 x 50 x 1.27 cm while the lower

Cerenkov counter was a 50 x 50 x 1.27 cm sheet of quartz placed inside

a white light collecting box. The scintillator, S1, was viewed by a

single 3" photomultiplier tube via an adiabatic light pipe connected to

one edge. The scintillator, S2, was viewed in a similar manner by two

3" photomultipliers. C1 was viewed via 4 adiabatic light guides by four

5" RCA 4525 photomultipliers while the C2 light box was viewed by 4 RCA

4522 photomultiplier tubes. The RCA 4522 tubes have windows of Corning 9741

ultraviolet transmitting glass and are well suited to viewing Cerenkov

light.

The use of a $BaSO_4$ white paint on the inside of the C2 diffusion box
made the box diffusely reflective to about 2200 A°. The charge section
also included an eight deck wire grid spark chamber with digital readout
(Enrmann et al., 1967). The spark chamber was used for trajectory deter-
mination and background removal. Trajectory information is necessary
in such a large area detector to make corrections for path length in the
various detector elements and to remove out of geometry events which may
trigger the experiment.

The electromagnetic cascade section comprised the region where electron-
initiated showers developed rapidly and were observed in sufficient detail
to estimate the energy of the incident electron and discriminate against
nuclear induced background events. This section consisted of eighteen
segments each of which was composed of a 50 x 50 x 0.64 cm plastic scin-
tillator and a 50 x 50 x 0.32 cm sheet of tungsten. Each of these segments
was viewed by two 3" photomultiplier tubes through air (non-adiabatic) light
guides. The outputs of the photomultipliers from each tungsten segment
were summed and pulse-height analyzed with the exception of the last two
pairs of tungsten segments where the outputs of the four photomultipliers
from each pair of segments were summed and pulse-height anlayzed.

Figure 1 shows the experiment configuration and the location of the
three "spray detectors" which sample the lateral shower development. Each
spray detector was a scintillator optically coupled to two 3" photomultiplier
tubes. The sum of the outputs of the pair of tubes on each of the spray
detectors were also pulse-height analyzed. The scintillator labelled SP1
was designed to sample backscatter from a shower. It was located at the
same height as the first tungsten segment (T1) but off to the side and

hence was outside the trigger geometry. Scintillator SP2 was located
on one side of the tungsten stack and it sampled leakage out of the
tungsten stack. It is similar in function to guard scintillators that
have been used by other experiments (Webber and Rockstroh, 1973; Marar
et al., 1971). The third spray scintillator, SP3, was located at the same
height as TOF2, the lower time-of-flight scintillator. SP3 was also
intended to sample the lateral shower properties. It should be noted that
none of the spray scintillators were included in the triggering require-
ments; thus no event was electronically rejected due to the pulse height
in any spray scintillator.

A time of flight system was also present on the experiment. Although
it was desirable to have the first detector element (C1) and the last
detector element T18) as the time-of-flight elements, this was not possible
because the existing photomultipliers on these detector elements were not
suitable for timing purposes and to install additional photomultipliers
would have required extensive modifications. Two additional timing scintill-
ators (TOF1 and TOF2) were added and were equipped with RCA 8575 photomultiplier
tubes having a 2 ns. rise time. One tube was mounted at the center of each
plastic scintillator. The output of each photomultiplier was fed to a time
to amplitude converter (TAC) which was pulse height analyzed to produce a
number related to the transit time of a particle from TOF1 to TOF2, a
distance of 108 cm. Cable lengths were adjusted so sea level muons passing
through the scintillators produced an output near channel 100 of the 256
channel pulse-height analyzer. This position for the downward moving
particle insured that an upward moving particle would also produce a pulse
height which was on scale.

The experiment triggering criteria were designed so an electron of

$\sim$ 7 GeV, would initiate an event readout. Above $\sim$ 9 GeV, the triggering

efficiency was nearly 100%. A detailed description of the triggering can

be found in previous publications (Silverberg et al., 1973, Ryan et al.,

1972, Crannell et al., 1973)

Flight five was launched from Cape Girardeau, Missouri on October 1,

1972. It was nearly stationary for more than 9 hours, then drifted less

than 200 miles from the launch site before landing. This flight lasted

for nearly 23 hours at a float altitude of 3.5 g/cm^2. Flight five

produced more data than the previous successful flights due to the higher

data rate (24 kilobits/sec), the smaller dead time, and the long duration.

A summary of the details of the flights is given in Table 1.

ANALYSIS OF FLIGHT DATA

Analysis of the flight data was begun by finding the particle

trajectories for each event. This was done by fitting the data from the

digital spark chamber to straight lines in the XZ and YZ planes (the

Z direction is the vertical through the experiment). If one and only one

"good" track was found in both the XZ and YZ projections, the event was

called a simple event. These events have an rms deviation from a straight

line of less than 0.15" or 1.5 wire spacings. In general, the deviation

is much smaller than this value (see Figure 2). All other events are

classified as complex and require different processing from the simple

events. In practice, the designation "complex event" meant that no single

well-defined track was obtained. On all balloon flights the complex events

accounted for about 60% of the events triggering the electron or e mode.

However, about 90% of the complex events were clearly not electron initiated,

as they had pulse-height profiles clearly incompatible with the accelerator

Table 1

Balloon Flights

	FLIGHT 3	FLIGHT 5
Launch Site	Alamagordo, N.M.	Cape Girardeau, Mo.
Vertical Cut-off Rigidity	5 GV	2.7 GV
Launch Date	Nov. 14, 1970	Oct. 1, 1972
Time at Float Altitude	14.5 hrs.	23 hrs.
Residual Atmosphere at Float Altitude	7.4 g/cm^2	3.5 g/cm^2
Fractional Live Time	0.42	0.55
Geometry Factor for Electrons in cm^2-ster	990±20	690±10

calibration results (Crannell et al., 1973; Whiteside et al., 1973). We postpone further discussion of the complex events until the analysis of the simple events are treated.

Although the triggering criteria limited the number of particles which the experiment analyzed, they represent only thresholds and hence alpha particles and other highly charged particles could initiate the e-mode triggering of the experiment. For this reason, a large number of the e-mode triggers had pulse-heights in the charge section which were too large for electron-initiated events. This background was eliminated by examining each e-mode event and checking its $S1$ and $C1$ (top Cerenkov counter) pulse-heights. If each pulse-height was less than 3 times the response to a sea-level muon and both were not greater than 2.5 times the muon response, the particle was accepted as singly-charged. These criteria were strict enough to insure that relativistic alpha particles were not accepted, yet singly-charged particles were not rejected. Once it was determined that a particle was singly-charged, its trajectory (as found by the spark chamber) was examined to be certain that the trajectory would pass inside of the inner 80% of the area of the last tungsten segment. This check assured that a well determined geometry was used and minimized edge effects.

The events which survived the above tests were fitted to the nominal value shower curve, $f(E_o, t_o, t_i)$ which gives the expected pulse height at depth t_i (in radiation lengths) when an electron of energy E_o starts to cascade at depth, t_o (Crannell et al., 1973). The fit is done by computing the quantity

$$(1) \qquad \chi^2 = \sum_{i=0}^{N} \left\{ \frac{f(E_o, t_o, t_i) - f_i}{\sigma(E_o, t_o, t_i)} \right\}^2$$

Here f_i is the observed normalized pulse height, $\sigma(E_o, t_o, t_i)$ is the standard deviation expected in $f(E_o, t_o, t_i)$ and N is the number of detectors used to sample the shower development.

Note that the function χ^2 in Equation (1) is defined in the same fashion as the familiar chi-square test frequently used in mathematics. In defining χ^2 in this way it was hoped that it would, in fact, have a chi-square distribution. Unfortunately, it does not because the distributions of fluctuations at each tungsten segment are not all Gaussian and it is not clear that all measurements at the tungsten segments are strictly independent (due to conservation of energy high fluctuations early in the shower tend to be followed by low fluctuations late in the shower and vice versa). The latter effect is probably not serious and most of the deviation from a chi-square distribution by the function χ^2 is due to the asymmetry of the shower fluctuations. Despite the lack of correlation with a chi-square distribution, the function χ^2 is an effective measure of the goodness of fit of an event to an electromagnetic cascade shower and can be used to determine the energy and apparent starting point of showering events as well as to discriminate against proton-initiated showers.

The analysis proceeded by selecting only apparent starting points, t_o, within one standard deviation of the maximum in the starting point distribution observed in calibration runs at the Stanford Linear Accelerator (SLAC). In this way the proton contamination was sharply reduced

and the fraction of electrons that was rejected in this way was restored

by a correction later in the analysis. For events with acceptable starting

points, the value of χ^2 was examined. If it was less than the χ^2 for 95%

of the electrons of energy E_o, the event was accepted as an electron.

The starting point and 95% criteria were somewhat arbitrary; they were a

compromise between keeping background down (trying to get all the electrons

greatly increased the proton background in the electron-like events) and

maintaining adequate statistics so the highest energy electron recorded

was limited only by the exposure factor.

CORRECTIONS

Although they are lumped into a single category, the complex events

actually fall into several distinct classes. These are shown in Table 2.

Type 1 and 3 events were the result of various types of background:

particles passing through light pipes or photomultiplier tube faces, pro-

ducing Cerenkov light, and then entering the experiment (this was possible

due to the very low thresholds in S1 and S2); showers starting above the

experiment where multiple particles are involved. This background was

nearly 20% of all the events. Examination of these events revealed no

Type 1 or 3 events which were even remotely electron-like. The Type 2

events were those where too few spark chamber coordinates were found for

reliable trajectory determination. This fraction (about 5%) was con-

sistent with the probability of less than five decks firing when the

efficiency of individual decks was considered.

Type 4 and 5 events were a much more common occurrence and probably

resulted from side-entering particles which interacted in the material

TABLE 2

COMPLEX EVENT CLASSIFICATION

1. No spark chamber data present (the chamber did not spark when pulsed). (less than 2%)

2. An insufficient number of decks fired for a reliable trajectory to be determined. (5%)

3. The trajectory found indicated the particle should not have triggered the experiment because the particle did not pass through the coincidence scintillators. (17%)

4. More than one acceptable trajectory was found. (20%)

5. No trajectory could be found which satisfied the least squares cutoff. (17%)

NOTE: Numbers in parentheses are the fraction of the events observed in each category.

around or in the experiment. The Type 4 and 5 events were the most
troublesome because the existence of multiple particles in the spark
chamber did not exclude the possibility that the initiating particle
was an electron, a result consistent with our accelerator data.
Since this possibility existed, it was important that these events be
studied carefully.

The most probable entry angle for particles triggering the electron
mode is 18-20°. The majority of the particles triggering the experiment
during a balloon flight are within about 10° of this mean angle. Thus,
one is never seriously in error by simply assuming the mean angle of
incidence for particles whose trajectory is not known. The Type 2, 4
and 5 events were thus analyzed by assuming that each particle was
incident on the experiment at the mean angle. The result of the
analysis was that 10% of the complex events were in all other respects
acceptable as electrons. The spectral index of these events was con-
sistent with that of the simple events and the flux was 58% of the flux
of the simple events.

To verify this procedure, the simple events were re-analyzed in the
same fashion as the complex events by ignoring the spark chamber data
and using the mean angle of incidence. As expected, this had little
effect on the spectral index, but it was found that the flux was 19%
higher than when the simple events were analyzed using the trajectory
data. This increase could be expected since the spark chamber data was
used to eliminate those simple events whose trajectories were near the
edges of the bottom of the experiment. Thus, ignoring the spark chamber

data effectively increased the geometry factor and hence increased the
apparent flux because a smaller geometry factor was used in the cal-
culation.

The analysis of the complex events and re-analysis of the simple
events described above showed that in addition to the electrons found
in the simple events there are 47 ±12% more electrons in the complex
events. Thus, to derive a correct absolute flux, a complex correction
of 1.47 ±0.12 had to be applied to the flux computed by using only the
simple events. This is equivalent to simply adding the fluxes from the
simple and complex events since it was found that the spectral indices
from the two types of events were the same.

The existence of the time of flight system gave additional infor-
mation on the complex events. It was found that the time of flight
distribution for all the complex events had a very large number of
events (about 40%) where times-of-flight were inconsistent with downward
moving particles. It was, however, found that the fraction of the
electron-like complex events with acceptable times of flight was con-
sistent with the fraction of the electron-like simple events (some of the
simple events did not have acceptable times of flight because the
geometry factor for the time of flight system was smaller than the
triggering geometry factor). Thus, the good correlation between simple and
complex electron-like events was consistent with the acceptance of
electron-like complex events as electrons.

Although the flights were at different geomagnetic cutoffs, it was
found that the e-mode trigger rate was consistent from one-flight to

another. This is because the instrument's own cutoff was higher than the local geomagnetic cutoff for electrons and contaminating hadrons which may masquerade as electrons are of much higher energy than the electrons they simulate. On this basis, the measured hadron contamination correction (Silverberg et al., 1973) of 29 ±5% was applied to the data from all flights.

TIME OF FLIGHT INFORMATION

Analysis of the time of flight data from flight five was carried out as a check on the previous flights where no time of flight data were available. There was an unresolved worry that some events initiated by side entering particles might look like electrons. If was felt that the spark chamber data enabled the effective elimination of this type of background; however, no independent check was handy. The results of the time of flight data on flight five indicated that the assumption of good rejection of the side-entering contaminant on all flights was correct.

The TOF was calibrated on sea-level muons. The spark chamber data was used to correct the raw data for light transit time from the particle's track in the scintillator to the photomultiplier tube. This resulted in a time resolution of ~ 0.9 ns FWHM. While this procedure worked well for sea-level muons, it was found that it was not applicable to showering events (i.e. most flight events). Especially for electrons, the tail of the shower is dominated by minimum attenuation gamma rays and their distribution is nearly isotropic deep in the shower. The particle or particles causing the stop signal in the TOF system could strike the

the bottom TOF scintillator almost anywhere. Thus, for showering particles it was not possible to correct for the distance from the bottom TOF photomultiplier tube to the particle causing the stop signal. This effect meant that time resolution was poorer for flight events than for the calibration muons.

The resolution, while poorer than for muons, was adequate to detect side-entering particles. Since most of the matter in the experiment was more than 48 cm from the top TOF scintillator, events having negative or nearly zero times of flight indicated side-entering particles. For singly charged e-mode triggers before any selection, there was evidence of this type of event. However, when a good fit to an electromagnetic shower was demanded, the contamination of these particles dropped to $\sim 12\%$, a fraction comparable to what would be expected due to the poor time resolution. Thus, the analysis of the TOF system confirmed our results on previous flights and indicated no significant contamination in the data from side-entering or bottom-entering particles.

SPRAY DETECTOR ANALYSIS

The spray detectors were also incorporated in this flight as a check on the procedures used in previous flights. As the flight five instrument was not recalibrated on accelerator electrons and protons after the spray detectors were installed, information presented here is based only on flight data and sea-level muon calibrations.

The spray detector information was analyzed by comparing the fraction of large pulse heights in each spray detector for all singly charged e-mode

triggers and for the electron-like events. Only events in which the trajectory of the incident particle would not pass through the respective spray scintillator were used. In each case, it was found that the fraction of the events where the pulse height in the spray detector exceeded two times minimum ionization was greater for the background e-mode events than for the electron-like events. The results are presented in Table 3.

TABLE 3

Fraction of Events Producing More Than Twice the Ionization
of a Sea-Level Muon in the Spray Scintillators

	SP1	SP2	SP3
electron-like events	2.6+.3%	8.9+.5%	12.8+.6%
singly charged e-mode events	10.5+.3%	17.1+.3%	27.0+.4%

Scintillator SP2 was positioned up against one face of the tungsten stack and is similar in function to guard scintillators used by other experimenters. While the assumption that background events have large pulse heights in this type guard scintillator appears to be borne out by these results, some caution is clearly warranted. When re-analyzing the electron-like events and demanding low SP2 pulse heights it was found that the spectrum was ~ 20% lower at ~ 10 GeV and 0.2 of a power steeper. Due to the large physical size of this experiment it may be that shower particles at low energies (~ 10 GeV) do not reach the spray scintillator as often as shower particles from the

higher energy events where the showers are wider and the number of shower particles is greater. This condition may not hold for some of the much smaller detectors that have flown and they may be rejecting a large fraction of the real electrons. Clearly, the 20% reduction may have to be multiplied by ~ 4 to simulate the effect of a guard counter sufficient to completely surround the cascade section. In this case, the reduction in the electron spectrum observed could be as much as 80%.

It has been suggested that backscattering from electromagnetic showers may become significant at high energies (Zatsepin, 1971; Orth, 1973). Such an effect might cause real electrons to be rejected as alpha particles at high energies. As a check on backscatter, the mean pulse height in S1 and C1 was examined by plotting these as a function of energy for the electron-like events. This plot is shown in Fig. 3. If backward-moving gamma-rays increased very rapidly with increasing energy, then a sharp rise would be apparent in this plot due to Compton electrons produced by the gamma rays. Although some rise is indicated, the observed effect is not large enough to cause any serious problem in the selection of singly-charged particles up to the energies reported here. Any attempt to extend the energy range of this instrument would have to deal with this effect more carefully.

The low fraction of events with large pulse heights in SP1 indicated that large angle backscatter occurred infrequencly. However, the large physical size of the experiment and the possible non-uniformity of the backscatter relative to the shower axis make application of these data to other experiments difficult.

The data from SP3 indicated that a spray detector at such a large
depth is not useful. Again the fraction should be multiplied by about 4
to 5 to approximate a fraction for a symmetric detector surrounding the
experiment at the same level. This gives ~ 65% for the fraction of
events having greater than twice minimum in this type detector com-
pared to ~ 100% for the background events. Other cutoffs .(three and
four times minimum) for discrimination were tried, but in no case did
the data from SP3 seem to be a strong discriminator between electron-
like and background events.

The results of this analysis of the spray detectors gave some in-
sight into their use by other experimenters and showed no inconsisten-
cies with the methods used here on the previous flights to select
electrons. As the differences between electrons and background events
were not great, the use of a guard detector on a large ionization
spectrometer would not appear to offer a significant improvement in
background rejection over the procedures used previously. These data
indicate that their use in smaller detectors should be carefully evalu-
ated and any significant improvement in   identification of individual
electrons beyond ~50 GeV may have to await the development of
detectors using advanced techniques (see e.g. Cherry et al., 1973).

RESULTS & DISCUSSION

The final results from the balloon flights are presented in Fig. 4
and Table 4. Flight five is somewhat lower in intensity at low energies
than the previous flight; the spectral index is also different, being

3.00 ±0.09 compared to 3.16 ±0.10 for the previous flights. The best
fit to all the data is provided by the power law spectrum

$$(2) \qquad \frac{dJ}{dE} = (430 \pm 110) \; E^{-3.10 \pm 0.08}$$

In Figure 5, the best fit to the data of this experiment and
the results of other workers have been plotted. There is clearly a
wide dispersion in experimental results. However, as pointed out
earlier, these results are derived from a variety of experimental and
analytic techniques in which systematic errors may play an important
role. The results of this experiment are in general agreement with
many workers near 10 GeV but drop off more quickly than the results of
Anand et al. (1973), and Scheepmaker and Tanaka (1971), to name but a
few.

While the spectral index reported here is close to that of Webber
and Rockstroh (1973), their intensity is considerably lower than
these data indicate. However, the Webber and Rockstroh experiment made use
of a guard counter and had a much smaller instrument than was used in
this experiment.

Note that near 10 GeV the balloon data is spread over a factor of
~ 5; however, two satellite experiments (Marsden et al., 1971;
Bleeker et al., 1970) which are not shown in Figure 5 are in good
agreement with these data near 10 GeV.

The dispersion at low energies (~ 10 GeV), where calibration can
be carried out and no extrapolations are necessary, are, perhaps,
more disturbing than the overall differences among the cosmic electron
measurements. Discrepancies may be due to poor proton rejection,

TABLE 4

Measured Differential Cosmic Ray Electron Spectrum
at the Top of the Atmosphere

	FLIGHT 3		FLIGHT 5
Energy GeV	Intensity Electrons/(m^2 ster sec GeV)	Energy GeV	Intensity Electrons/(m^2 ster sec GeV)
11.7	$(2.5 \pm 0.45) \times 10^{-1}$	11.6	$(2.2 \pm 0.40) \times 10^{-1}$
15.6	$(1.1 \pm 0.20) \times 10^{-1}$	15.5	$(8.0 \pm 1.4) \times 10^{-2}$
21.0	$(4.9 \pm 0.88) \times 10^{-2}$	20.8	$(3.1 \pm 0.56) \times 10^{-2}$
28.3	$(1.8 \pm 0.32) \times 10^{-3}$	28.3	$(1.1 \pm 0.20) \times 10^{-3}$
37.9	$(6.5 \pm 1.2) \times 10^{-3}$	38.5	$(4.8 \pm 0.91) \times 10^{-3}$
51.1	$(2.3 \pm 0.51) \times 10^{-3}$	51.4	$(2.2 \pm 0.44) \times 10^{-3}$
68.7	$(1.1 \pm 0.26) \times 10^{-3}$	69.8	$(8.3 \pm 1.7) \times 10^{-4}$
92.1	$(3.8 \pm 1.1) \times 10^{-4}$	92.8	$(4.2 \pm 1.0) \times 10^{-4}$
122.0	$(7.0 \pm 3.7) \times 10^{-5}$	123.0	$(1.8 \pm 0.50) \times 10^{-4}$
171.0	$(5.2 \pm 2.8) \times 10^{-5}$	179.0	$(7.2 \pm 2.4) \times 10^{-5}$
		233.0	$(9.0 \pm 6.7) \times 10^{-6}$

application of criteria which eliminate electrons in an attempt to
reduce the proton background, problems due to poor energy estimation,
and the application of other corrections.

In comparing the data of one experiment to another several points
should be kept in mind:

(1) Errors in energy of as little as 10% can result in absolute
flux errors of $\sim$ 30% due to the steep slope of the electron spectrum.

(2) The use of guard counters may severely reduce the absolute
flux and may affect the spectral index.

(3) Additional and more uncertain corrections are required to
derive an absolute flux than to derive the relative flux.
For these reasons, the fact that much of the experimental data do not
agree within a few times the estimated errors may not be as significant
as it appears and the differences in slope reported indicate more
serious discrepancies in measured results.

In comparing these data with other results it should be remembered
that while many experiments compensate for proton contamination, we
know of no other experiment where the residual proton contamination
was actually measured (Silverberg et al., 1973). This was possible
only because of the great depth of the instrument used in flight three.

The good statistics obtained in this experiment have also been
exploited in an attempt to verify the results or at least find that
they are self-consistent. The spectrum of singly charged e-mode
events whose starting points were within 0.2 radiation lengths of
the peak in the electron starting point distribution as measured in

calibration runs (see Figure 6) was found. By choosing events from
the region where electrons are most dense, the electron to proton
ratio is maximized. The spectral index observed was 3.3 ± 0.2 for
this subset of events. The steep spectrum in this region is thus consistent
with the results using all the data. The loss in this analysis is,
of course, statistics and therefore the spectrum cannot go to as high
an energy as when using all the data.

In an analogous fashion, the spectrum was computed for only
those singly charged e-mode events which fit extremely well to electro-
magnetic showers. The acceptance criteria were tightened to the point
where only 50% of the accelerator electrons would have been accepted.
Again this severely discriminated against protons at the expense of
statistics and the result was again a steep spectrum with index 3.2 ± 0.2.

Both of these tests indicate that a steep spectrum is called for
and are suggestive that if the spectrum reported here is in error it
may be too flat rather than too steep.

A further check on the results was performed by examining the
spectrum of the e-mode triggers that were not electron-like. These
events should have been predominantly protons. While the fitting of
electromagnetic showers to proton events results, in general, in poor
agreement in the detail of the showers, the proton calibration
done at the Brookhaven AGS indicated that the best fit energy was
porportional to the true proton energy (see Whiteside et al., 1973).
Thus, simply using the best fit energy for these proton events should
give a spectral index like the proton index even though the magnitude

of the flux is in error. When the computation was carried out, the spectral index was 2.7 ± 0.1, in agreement with the high energy proton spectral index (Ryan et al., 1972).

The electron flux reported here is considerably higher than could be expected from a secondary origin of the cosmic electron assuming that the cosmic ray nuclei pass through ~5 g/cm^2 (Shapiro and Silberberg, 1970). Thus, no large fraction of the cosmic electrons can be of secondary origin. This conclusion is consistent with the electron charge composition measurements (DeShong et al., 1964; Hartman, 1967; Buffington et al., 1974) and the conclusions of many other experimenters.

Based on the leakage lifetime approximation, the spectral index of the electron flux is expected to steepen by a full power due to synchrotron and inverse Compton losses. This approximation has been called into question by Jokipii and Meyer (1968) because it replaces the diffusion term in the transport equation by a characteristic loss term. Under the assumption of isotropic diffusion with a disk-shaped source region, Jokipii and Meyer find a spectrum with two "breaks", each of one-half a power, at energies separated by a factor of ~ 50, depending on the dimensions of the source region. On the other hand, Berkey and Shen (1969) have carried out a similar treatment using convection diffusion and find that the results are similar to the leakage lifetime model with only one break occurring. This model does not include the effects of perpendicular diffusion or the role of the random magnetic field lines in allowing escape from the disk. Berkey and Shen and Webster (1970) concluded that the source distribution may

be more important in determining the equilibrium spectrum than the propagation or boundary conditions. Webster, in fact, claims that by postulating a proper distribution of sources, an arbitrary break can be achieved.

Since the electron spectral index obtained here is approximately one-half power steeper than the proton spectral index, the Jokipii and Meyer model seems attractive; however, Jones (1970) has shown that even in the leakage lifetime model the change in spectral index of one power takes place over more than a decade in energy. Webster has commented that even this broad range in energies where the spectral index is changing may be enlarged further by geometric effects of the source region if the observer is not near the center of the source distribution. Thus, unless the turnover occurred below 10 GeV, some evidence of a changing slope might be expected in these data.

In interpreting the results of this experiment, we consider what the expected electron spectrum is in the measured energy range using the simplest model. Ramaty (1974) has shown that for a power law source spectrum, $Q(E) = AE^{-\Gamma_0}$, the equilibrium density of electrons is given by

$$(3) \qquad N(E) = AE^{-\Gamma_0} \int_0^\infty \frac{1}{bE} (1-bE_x)^{\Gamma_0 - 2} e^{-\frac{x}{\tau}} P_0(x) \, dx$$

where the energy loss rate is

$$(4) \qquad -\frac{dE}{dt} = bE^2$$

and

(5) $b = (4 \times 10^{-6} H_{\perp}^{2} + 4 \times 10^{-19} T_{bb}^{4})$ $(\text{GeV-sec})^{-1}$

$H_{\perp}$ is the mean magnetic field perpendicular to the electron's motion in gauss and T_{bb} in the temperature of the universal blackbody radiation in °K, $P_{0}(x)$ is a function dependent on the propagation of the electrons and boundary conditions. For the simplest case, $P_{0}(x) = 1$, and the exponential lifetime distribution results. This is equivalent to the leakage lifetime approximation with lifetime τ.

In Figure 7, the resulting electron spectrum is shown in the energy range 1-1000 GeV. The spectrum was computed using $H_{\perp} = 4 \times 10^{-6}$ gauss, $\tau = 3 \times 10^{6}$ years, and $T_{bb} = 2.8°K$. These are reasonable current estimates of the magnetic field in the galactic disk and the temperature of the blackbody radiation. The escape lifetime was chosen to agree with the estimates from the fragmentation of the nuclear component of cosmic rays (Shapiro and Silberberg, 1970) and isotopic studies (Webber et al., 1973).

While the spectrum does indeed turn down in this energy region, the change in slope is so gradual as to be nearly imperceptible if one were to examine only a single decade in energy. Since these experimental data span from 10 to ~ 200 GeV, ten equally-spaced points in that energy interval were taken on the theoretical curve and these were fitted to a power law spectrum. Both the theoretical electron spectrum and the best fit to a power law are shown in Figure 8.

The best fit power law has a spectral index of 3.11, in surprisingly excellent agreement with these experimental results. The curve is changing slope so slowly that the power law fit is adequate when experimental uncertainties are attached to each point. Thus, it

is impossible to positively detect the curvature in the data from such a restricted energy range and the only indication of the changing slope is the seemingly peculiar spectral index.

While a simple numerical agreement certainly does not prove a theory, we conclude that these data do not rule out the predictions of the leakage lifetime model. It is also clear that more exotic models involving complicated diffusion and elaborate boundary conditions are not necessary until better experimental data are available to allow these possibilities to be distinguished from the simple leakage lifetime model. To resolve such questions, large area detectors capable of positive identification of individual electrons (and, hopefully, negatron and positron separation) are needed. These detectors should be flown for long periods of time, preferably on satellites where no atmospheric corrections need be applied. Satellites might also be able to measure anisotropy in the cosmic electrons (Earl and Lenchek, 1969; Shen and Mao, 1971). In this way it should be possible to extend our knowledge of the cosmic electron spectrum above 10^4 GeV and resolve some of the questions concerning details of the sources of electrons and their propagation through space.

The experiment described here has shown that excellent energy resolution and good proton rejection can be achieved by frequent sampling of electromagnetic cascades. On one flight it was shown that a very deep detector is valuable in detecting protons which may simulate electrons; however, the proton separation was statistical with the exception of a small fraction of the data on one flight.

These experiments have provided data over more than a decade in energy with the dominant errors being systematic ones and not statistical. The results of the flights have shown that the cosmic electron energy spectrum above 10 GeV is steeper than previously thought having a spectral index of ~ 3.1, significantly different from the proton spectral index at high energies.

FIGURE CAPTIONS

Figure

1.   Experiment configuration for Flight Five.

2.   Distribution of spark chamber least squares fit errors.

3.   Mean response in muon equivalents of the charge determination
      detectors versus estimated energy of the incident electron.
      Error bars represent one standard deviation for a single event,
      while points are average values.

4.   Differential cosmic ray electron spectrum measured in this
      experiment and best fit power law.

5.   Recent measurements of the differential spectrum of primary
      cosmic ray electrons and comparison with this experiment.

6.   Distribution of the apparent starting points for events
      initiated by SLAC electrons.

7.   Theoretical differential spectrum of cosmic ray electrons in the
      leakage lifetime model (arbitrary normalization).

8.   Theoretical differential spectrum of the cosmic ray electrons
      in the leakage lifetime model compared to best fit power law
      to points chosen from the theoretical curve.

REFERENCES

Anand, K. C., R. R. Daniel and S. A. Stephens, "Final Results on the
        TIFR Cosmic Ray Electron Spectrum in the Region 10 to 800 GeV",
        Conference Papers, 13th Int. Cosmic Ray Conf., Int. Union of
        Pure and Applied Physics, Denver, Colorado 1, 355, 1973.

Berkey, G. B. and C. S. Shen, "Origin and Propagation of Cosmic-Ray
        Electrons", Phys. Rev. 188, 1994, 1969.

Bleeker, J. A. M., J. J. Burger, A. J. M. Deerenberg, H. C. Van de Hulst,
        A. Scheepmaker and B. N. Swanenburg, "The Cosmic Ray Electron
        Spectrum Between 0.5 and 10 GeV Observed on Board OGO-5",
        Acta Phys. Acad. Scient. Hung. 29 Suppl. 1, 217, 1970.

Buffington, A., C. D. Orth, and G. F. Smoot, "A Measurement of the
        Positron-Electron Ratio in the Primary Cosmic Rays from 5 to
        50 GeV", Phys. Rev. Lett. 33, 34, 1974.

Cherry, M. L., D. Müller and T. A. Prince, "The Efficient Identification
        of Relativistic Particles by Transition Radiation", Conference
        Papers, 13th Int. Cosmic Ray Conf., Int. Union of Pure and
        Applied Physics, Denver, Colorado 5, 3261, 1973.

Crannell, C. J., R. A. Gearhart, F. A. Hagen, W. V. Jones, R. J. Kurz,
        J. F. Ormes, R. D. Price, R. F. Silverberg and G. M. Simnett,
        "Electron Calibration of a high-energy Cosmic Ray Detector",
        Nucl. Instrum. Methods 108, 445, 1973.

De Shong, J. A., R. H. Hildebrand and P. Meyer, "Ratio of Electrons to
        Positrons in the Primary Cosmic Radiation", Phys. Rev. Lett. 12,
        3, 1964.

Earl, J. A. and A. M. Lenchek, "Are Cosmic Electrons Anisotropic?",
        Astrophys. J. 157, 87, 1969.

Earl, J. A., D. E. Neely and T. A. Rygg, "Balloon Measurements of the
        Energy Spectrum of Cosmic Electrons between 1 and 25 GeV",
        J. Geophys. Res. 77, 1087, 1972.

Ehrmann, C. H., C. E. Fichtel, D. A. Kniffen and R. W. Ross, "A Magnetic
        Core Digitized Spark Chamber for Space Science Experiments",
        Nucl. Instrum. Methods 56, 109, 1967.

Hartman, R. C., "The Energy Dependence of the Positron-Electron Ratio
        in the Primary Cosmic Radiation in 1965", Astrophys. J. 150,
        371, 1967.

Jokipii, J. R. and P. Meyer, "Storage and Diffusion of Cosmic-Ray
        Electrons in the Galaxy", Phys. Rev. Lett. 20, 752, 1968.

Jones, F. C., "Cosmic Ray Diffusion and the Leakage Lifetime
        Approprimation: An Investigation of its Validity by the
        Eigenfunction Expansion Technique", Phys. Rev. D2, 2787, 1970.

Marar, T. M. K., P. S. Freier and C. J. Waddington, "Intensity and
        Energy Spectrum of Energetic Cosmic Ray Electrons", J. Geophys.
        Res. 76, 1625, 1971.

Marsden, P. L., R. Jakeways and I. R. Calder, "Primary Electron
        Observations (3≤E≤15 GeV) Recorded on the ESRO II Satellite",
        12th Int. Conf. on Cosmic Rays, Int. Union of Pure and Applied
        Physics, Hobart, Tasmania, Australia, 1, 110, 1971.

Müller, D. and P. Meyer, "The Spectrum of Galactic Electrons with
        Energies Between 10 and 900 GeV", Astrophys. J. 186, 841, 1973.

Nishimura, J., E. Mikumo, I. Mito, K. Niu, I. Ohta and I. Tiara,
        "Observation of the Electron Component in Cosmic Rays with
        Emulsion Chamber", paper presented at 11th Int. Conf. on Cosmic
        Rays, Int. Union Pure Applied Phys., Budapest, Aug. 25-Sept. 4,
        1969.

Orth, C. D., private communication, 1973.

Ramaty, R., Chapter III in High Energy Particles and Quanta in
        Astrophysics, ed. F. B. McDonald and C. E. Fichtel, MIT Press,
        Cambridge, Mass., 1974.

Ryan, M. J., J. F. Ormes and V. K. Balasubrahmanyan, "Cosmic-Ray
        Proton and Helium Spectra above 50 GeV", Phys. Rev. Lett. 28,
        985, 1972.

Scheepmaker, A. and T. Tanaka, "Primary Cosmic-Ray Electron Spectrum
        between 5 and ∼ 300 GeV in 1968", Astron. and Astrophys. 11,
        53, 1971.

Shapiro, M. M. and R. Silberberg, "Heavy Cosmic Ray Nuclei", Ann. Rev.
        Nucl. Sci. 20, 323, 1970.

Shen, C. S. and C. Y. Mao, "Anisotropy of High Energy Cosmic Electrons
        in the Discrete Source Model", Astrophys. Letters 9, 169, 1971.

Silverberg, R. F., J. F. Ormes and V. K. Balasubrahmanyan, "Primary
        Cosmic Ray Electrons above 10 GeV: Measurements Using a Thick
        Detector", J. Geophys. Res. 78, 7165, 1973.

Webber, W. R., "The Energy Spectra of the Cosmic Ray Nucleonic and Electronic Components", Conference Papers, 13th Int. Cosmic Ray Conf., Int. Union of Pure and Applied Physics, Denver, Colorado 5, 3568, 1973.

Webber, W. R., J. A. Lezniak, J. Kish and S. V. Damle, "The Relative Abundance of the Isotopes of Li, Be and B and the Age of Cosmic Rays", Astrophys. & Space Sci. 24, 17, 1973.

Webber, W. R. and J. M. Rockstroh, "Cosmic Ray Electrons with E > 1 GeV -- Some New Measurements and Interpretations", J. Geophys. Res. 78, 1, 1973.

Webster, A. S., "On the Diffusion-Loss Model of Cosmic Ray Electron Propagation in the Galaxy", Astrophys. Letters 5, 189, 1970.

Whiteside, H., C. J. Crannell, H. Crannell, J. F. Ormes, M. J. Ryan and W. V. Jones, "Energy Calibration of a Cosmic Ray Ionization Spectrometer", Nucl. Instrum. Methods, 109, 375, 1973.

Zatsepin, V. I., "The Electron Energy Spectrum in the Galactic Cosmic Ray Flux in the Region 5 - 600 GeV", 12th Int. Conf. on Cosmic Rays, Int. Union of Pure and Applied Physics, Hobart, Tasmania, Australia, 1, 116, 1971.

FLIGHT 5
EXPERIMENT CONFIGURATION
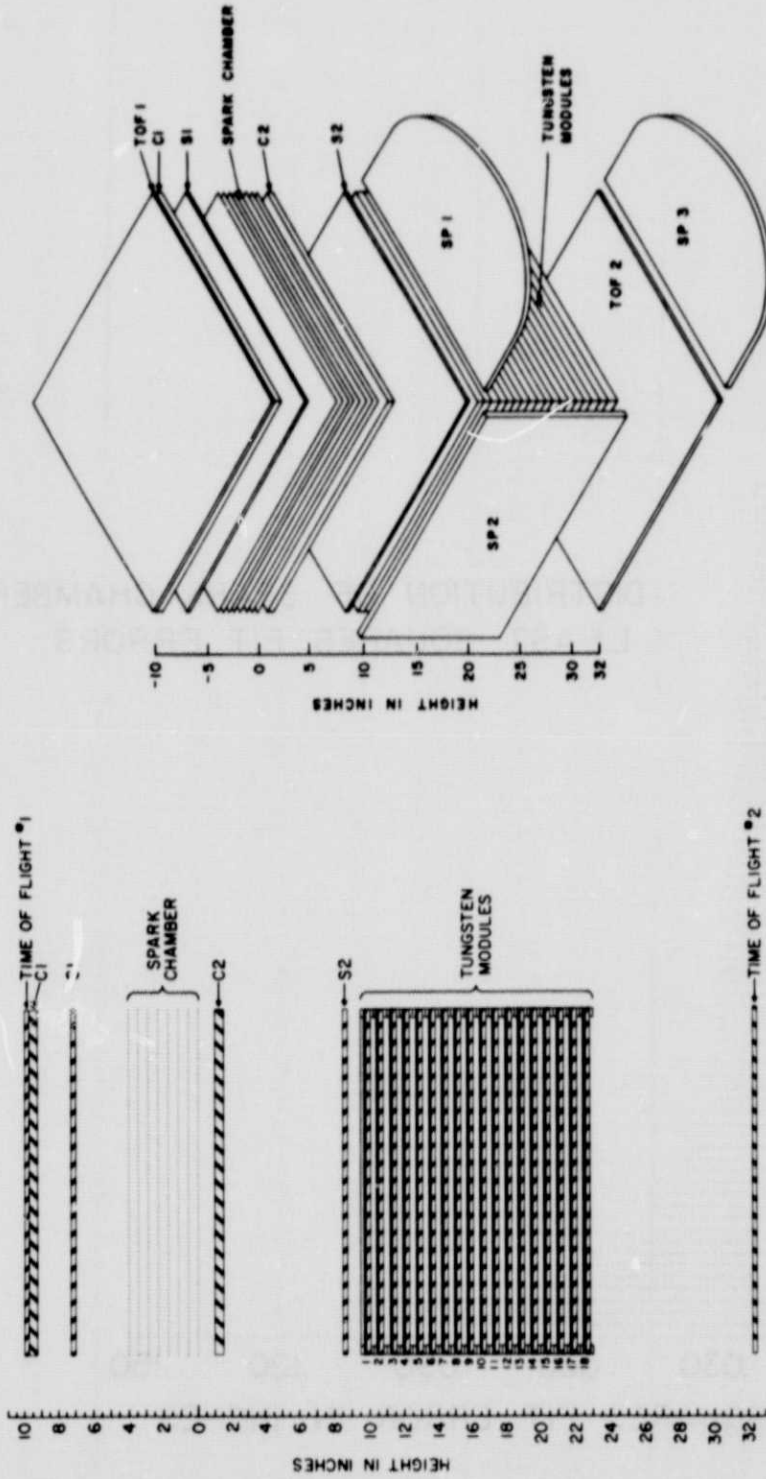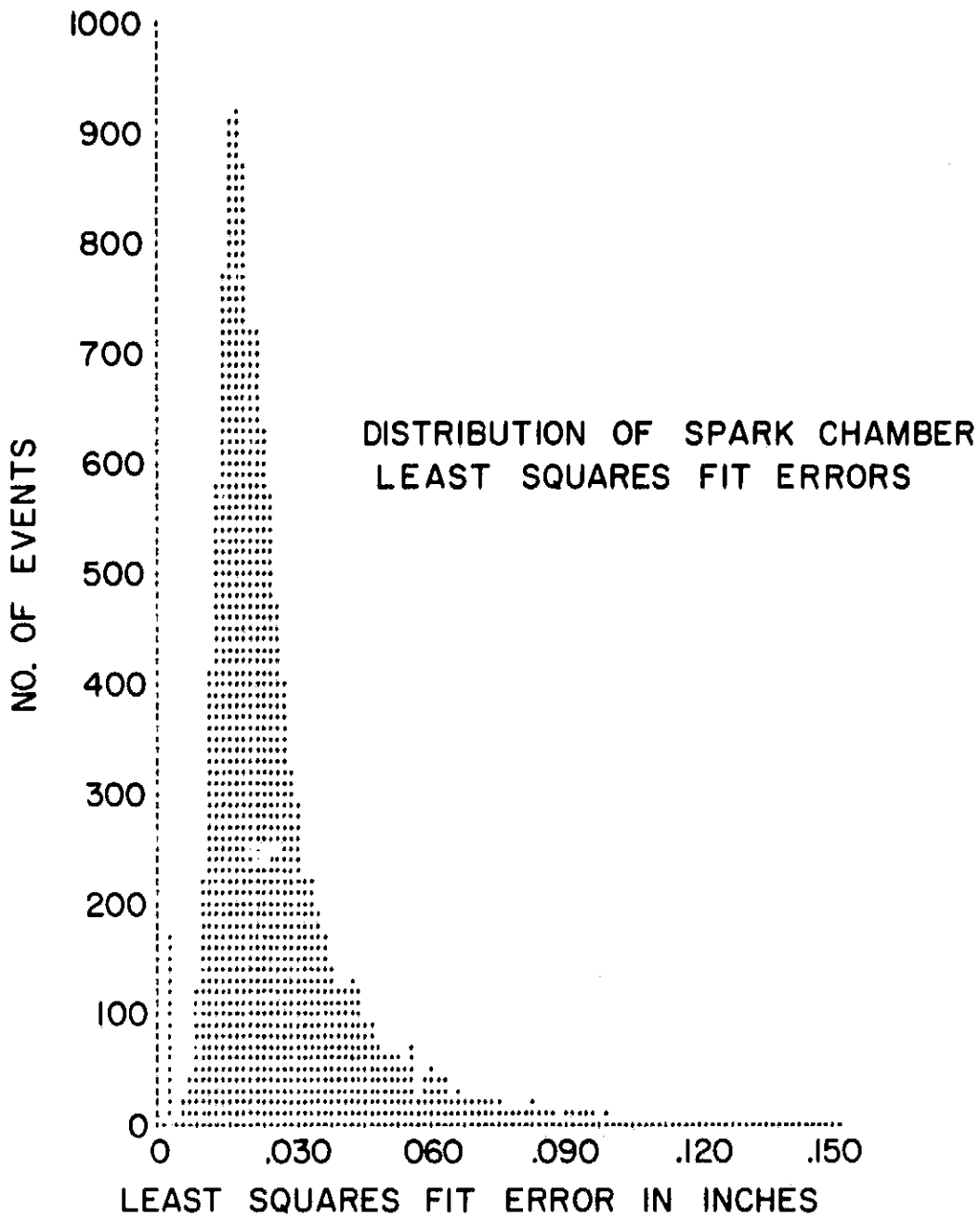
Fig. 1. Experiment configuration
for Flight Five.

Fig. 2. Distribution of spark
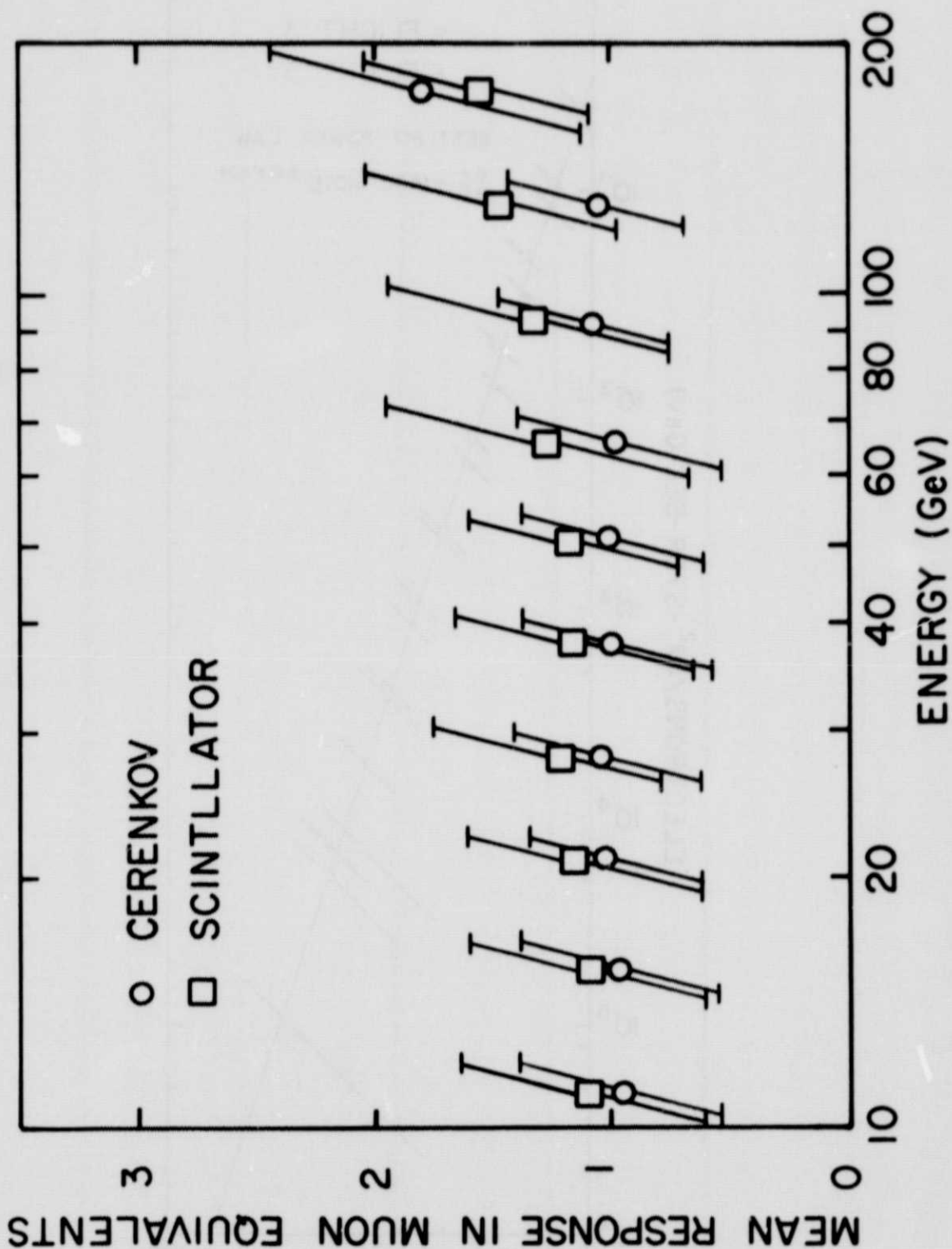chamber least squares fit errors.

Fig. 3. Mean response in muon equivalents of the charge determination detectors versus estimated energy of the incident electron. Error bars represent one standard deviation for a single event, while points are average values.
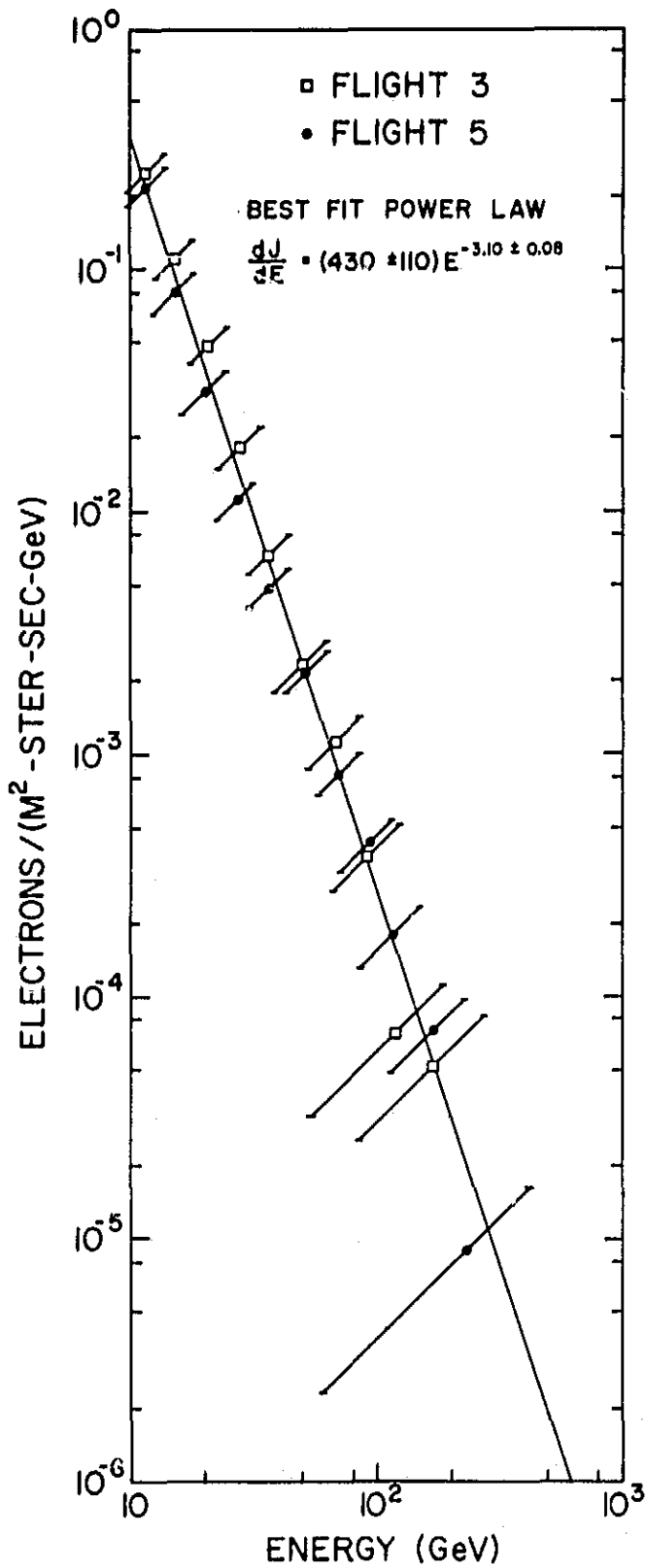
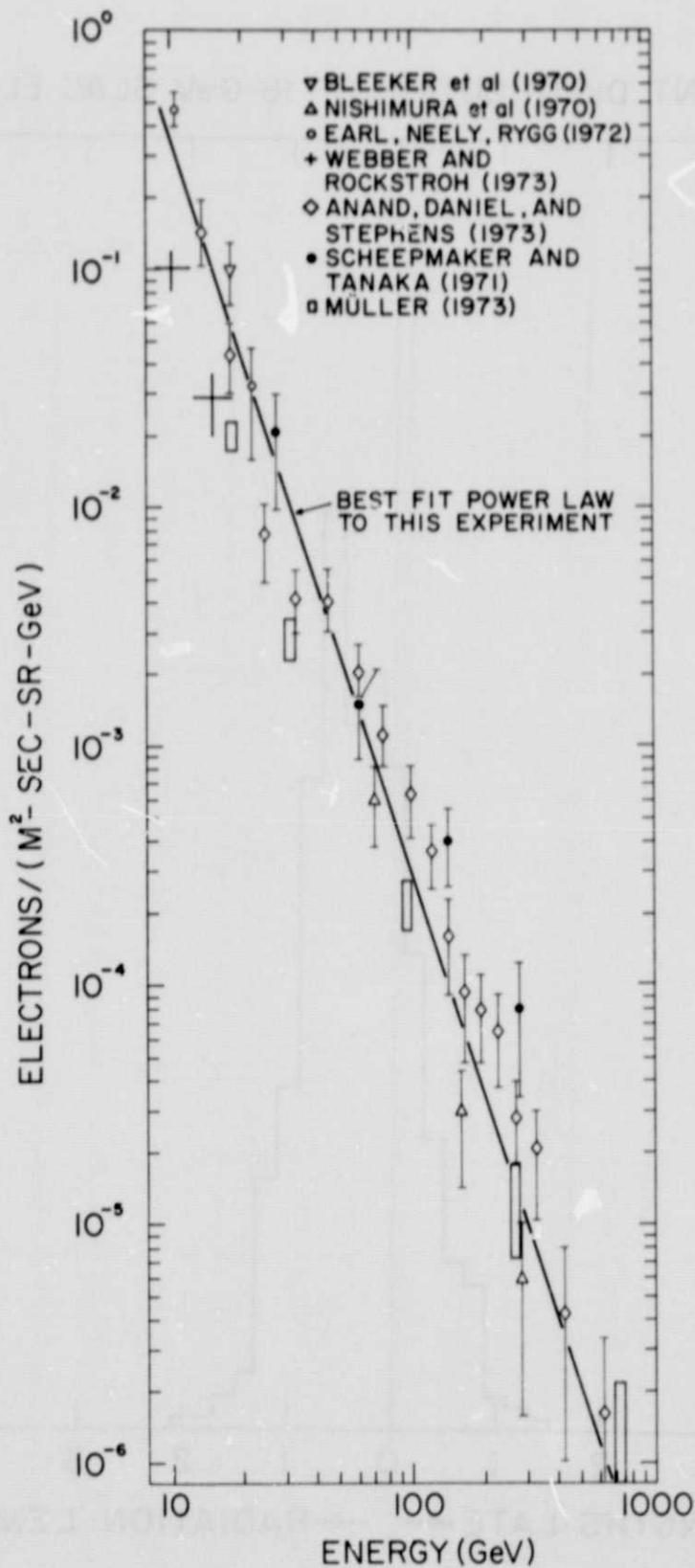Fig. 4. Differential cosmic ray electron spectrum measured in this experiment and best fit power law.

Fig. 5. Recent measurements of the differential spectrum of primary cosmic ray electrons and comparison with this experiment.

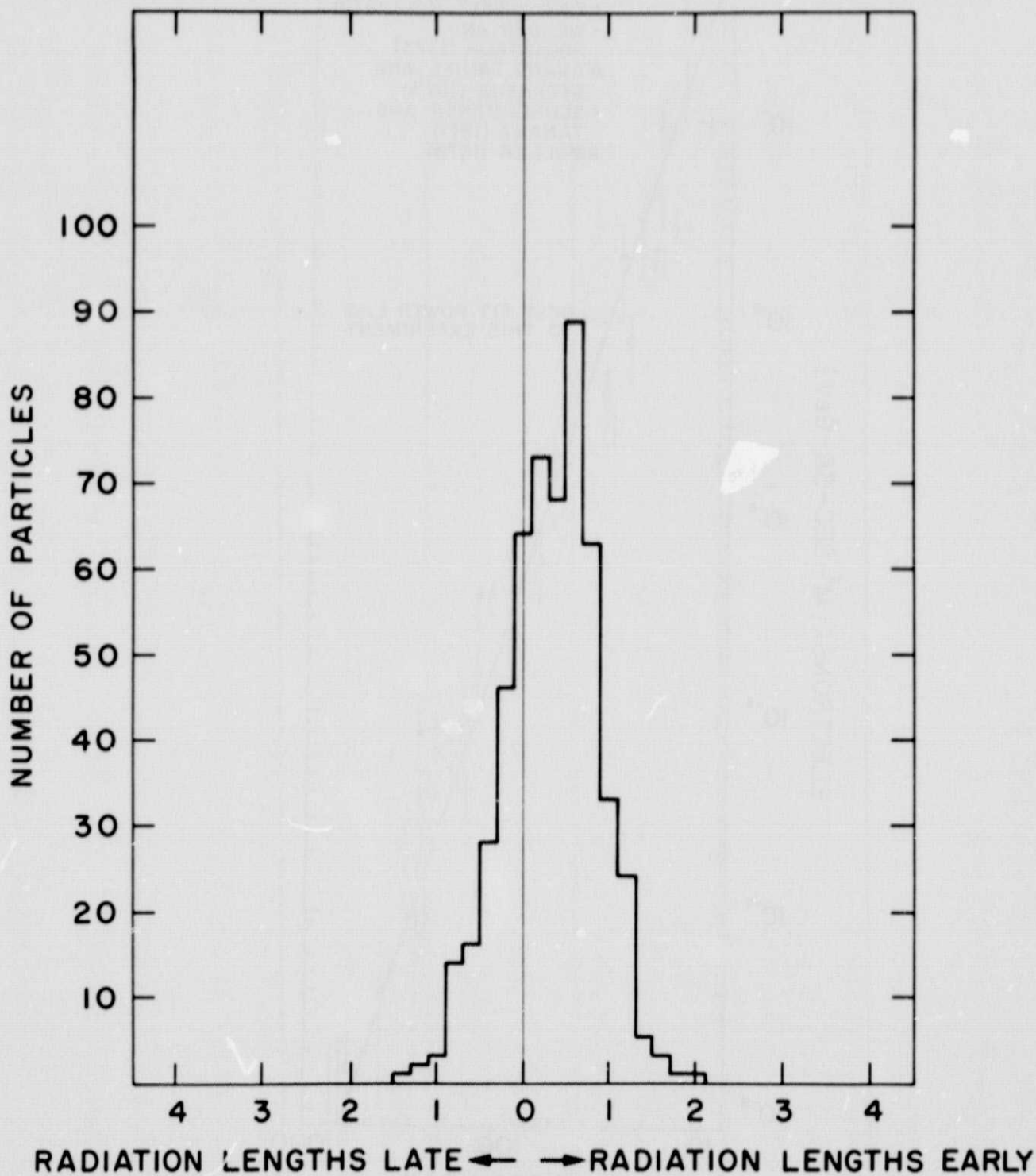# STARTING POINT DISTRIBUTION OF 16-GeV SLAC ELECTRONS

Fig. 6. Distribution of the apparent
starting points for events initiated
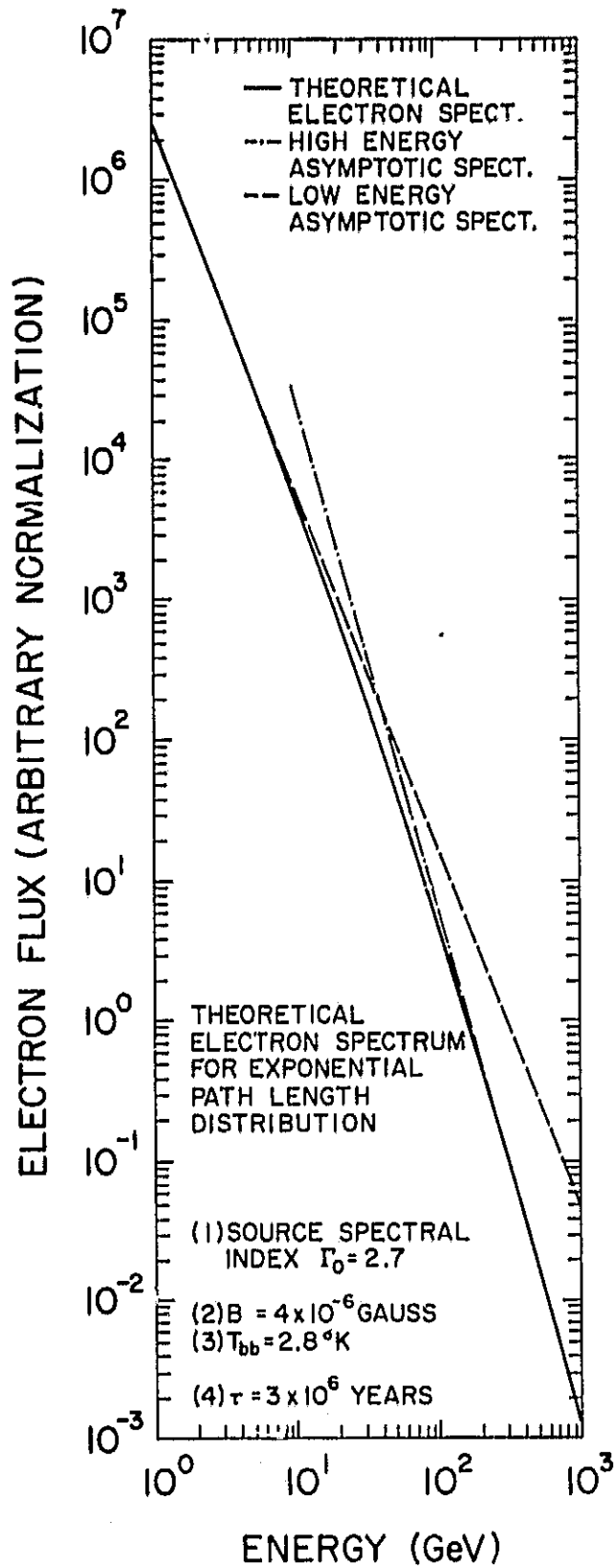by SLAC electrons.

Fig. 7. Theoretical differential spectrum of cosmic ray electrons in the leakage lifetime model (arbitrary normalization).
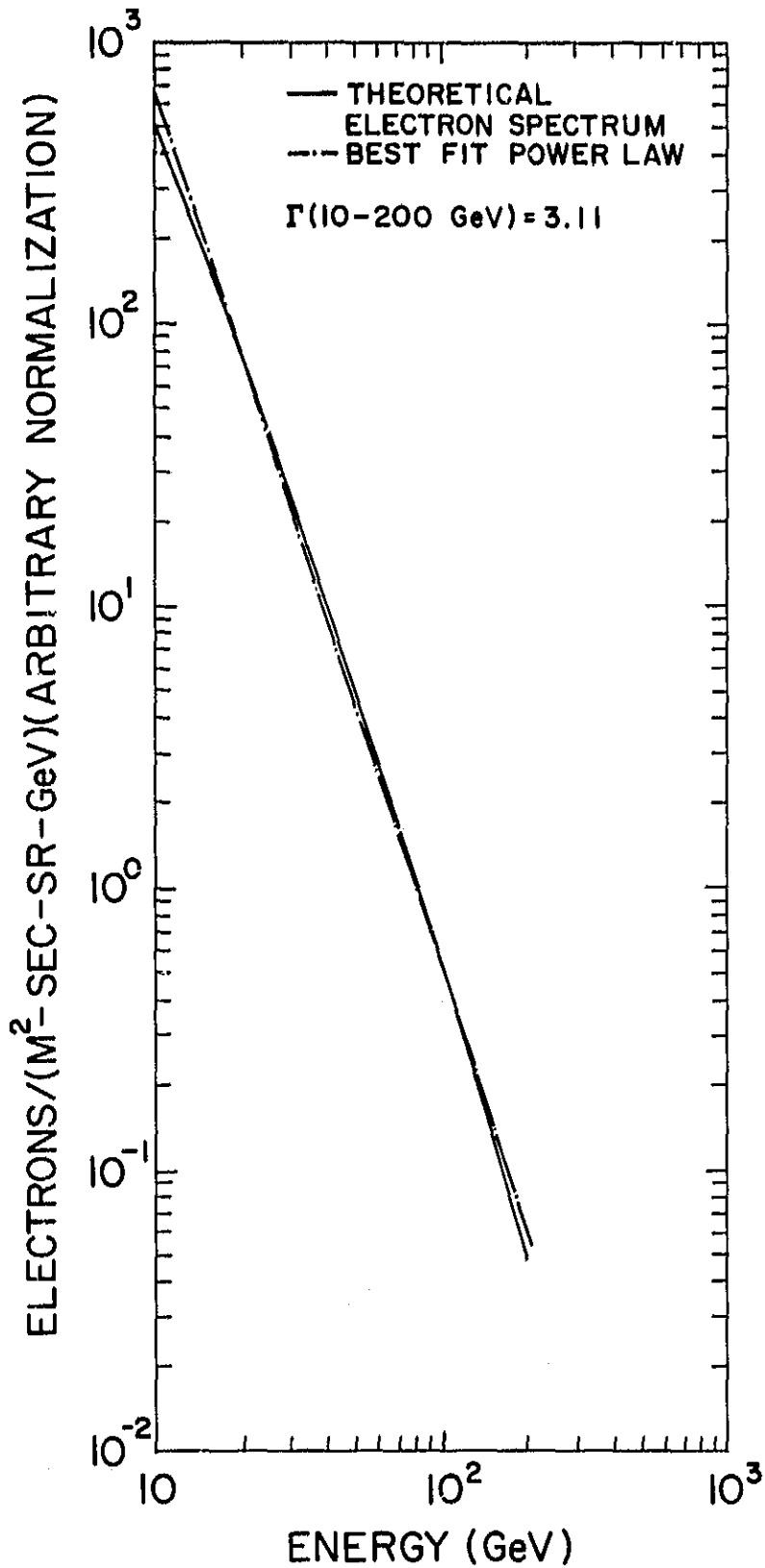
Fig. 8. Theoretical differential
spectrum of the cosmic ray electrons
in the leakage lifetime model compared
to best fit power law to points chosen
from the theoretical curve.